Complementary metal--oxide--semiconductor compatible high efficiency subwavelength grating couplers for silicon integrated photonics

ARTICLE *in* APPLIED PHYSICS LETTERS · JULY 2012

Impact Factor: 3.3 · DOI: 10.1063/1.4737412

6 AUTHORS, INCLUDING:

Xiaochuan Xu
University of Texas at Austin
73 PUBLICATIONS **434** CITATIONS
SEE PROFILE

John Covey
21 PUBLICATIONS **124** CITATIONS
SEE PROFILE

David Kwong
University of Texas at Austin
43 PUBLICATIONS **244** CITATIONS
SEE PROFILE

Ray T Chen
University of Texas at Austin
676 PUBLICATIONS **5,665** CITATIONS
SEE PROFILE

AIP | Applied Physics Letters

Complementary metal–oxide–semiconductor compatible high efficiency subwavelength grating couplers for silicon integrated photonics

Xiaochuan Xu, Harish Subbaraman, John Covey, David Kwong, Amir Hosseini et al.

Citation: Appl. Phys. Lett. **101**, 031109 (2012); doi: 10.1063/1.4737412
View online: http://dx.doi.org/10.1063/1.4737412
View Table of Contents: http://apl.aip.org/resource/1/APPLAB/v101/i3
Published by the American Institute of Physics.

Related Articles

Silicon nanomembrane based photonic crystal waveguide array for wavelength-tunable true-time-delay lines
Appl. Phys. Lett. 101, 051101 (2012)

Demonstration of low-loss on-chip integrated plasmonic waveguide based on simple fabrication steps on silicon-on-insulator platform
Appl. Phys. Lett. 101, 041117 (2012)

Efficient and broadband polarization rotator using horizontal slot waveguide for silicon photonics
Appl. Phys. Lett. 101, 021105 (2012)

Trapping of surface plasmon waves in graded grating waveguide system
Appl. Phys. Lett. 101, 013111 (2012)

Quantitative analysis and near-field observation of strong coupling between plasmonic nanogap and silicon waveguides
Appl. Phys. Lett. 100, 231109 (2012)

Additional information on Appl. Phys. Lett.

Journal Homepage: http://apl.aip.org/
Journal Information: http://apl.aip.org/about/about_the_journal
Top downloads: http://apl.aip.org/features/most_downloaded
Information for Authors: http://apl.aip.org/authors

ADVERTISEMENT

Complementary metal–oxide–semiconductor compatible high efficiency subwavelength grating couplers for silicon integrated photonics

Xiaochuan Xu,[1,a),b)] Harish Subbaraman,[2,a)] John Covey,[1] David Kwong,[1] Amir Hosseini,[2] and Ray T. Chen[1,b)]
[1]*Department of Electrical and Computer Engineering, The University of Texas at Austin, Austin, Texas 78712, USA*
[2]*Omega Optics, Inc., 10306 Sausalito Dr., Austin, Texas 78759, USA*

(Received 18 May 2012; accepted 1 July 2012; published online 18 July 2012)

We demonstrate a through-etched grating coupler based on subwavelength nanostructure. The grating consists of arrays of 80 nm × 343 nm rectangular air holes, which can be patterned in a single lithography/etch. A peak coupling efficiency of 59% at 1551.6 nm and a 3 dB bandwidth of 60 nm are achieved utilizing the silicon-on-insulator platform with a 1 μm thick buried-oxide layer for transverse electric mode. The performance is comparable to gratings requiring much more complicated fabrication processes. © *2012 American Institute of Physics*. [http://dx.doi.org/10.1063/1.4737412]

Silicon photonics has been considered a promising platform for high density integration of optoelectronic devices.[1,2] The high index contrast between silicon and its cladding materials (air, silicon dioxide, etc.) allows for the fabrication of submicron structures such as single mode waveguides, resonators, photonic crystals, etc. However, coupling light into and out of these devices through fiber butt coupling suffers from high losses induced by the large mode and effective index mismatches between fiber and strip waveguides with submicron cross sections. The reported efficient coupling schemes include end-fire coupling and off-surface coupling.[3] The inverse taper, proposed in 2002,[4] has been proved to be an effective solution for end-fire coupling. The highest coupling efficiency demonstrated so far is ~0.5 dB for transverse electric (TE) polarization.[5] The strip waveguide tip must be sufficiently narrow (e.g., 30 nm (Ref. 5)) to stimulate a delocalized mode. As a result, the height-to-width aspect ratio of the tip is so high that the lithography becomes challenging resulting in a low yield. Furthermore, the resulting mode spot size is still much smaller than that of a single mode fiber, and a lensed fiber is needed to further ameliorate mode matching.[6,7] In many cases, the chip needs to be diced and polished, so that the distance from the nano-taper tip to the chip edge becomes ~3 μm or less.[7] These crucial requirements limit the application of inverse tapers. To overcome these limitations, a subwavelength edge coupler was proposed,[8] and a 0.9 dB coupling efficiency was demonstrated experimentally.[9] The taper width increases to 300 nm, and there is no need for high precision termination at the cleaved chip edge. However, a lensed fiber is still necessary. An alternative solution for achieving high fiber-to-chip coupling efficiencies is the use of a grating coupler (GC).[10–12] Initial efforts in 2006 exhibited a coupling efficiency of 37% and a 1 dB bandwidth of 40 nm.[10] The grating required two etches, one of which is a 70 nm shallow etch.[10] Subsequently, the addition of an epitaxial silicon overlay enhanced emission directionality to the fiber, thereby increasing the efficiency to 55%.[12] The fabrication process contained as many as eight steps, including two etches and an epitaxial growth. The directionality may be further improved using a bottom reflector,[10,13] but fabrication complexity would significantly increase as well. Using the lag effect of reactive ion etching (RIE), a 64% coupling efficiency was also recently demonstrated,[11] but the fabrication also involved two etches.

Thus, experimentally demonstrated GCs usually demand complex fabrication processes. Despite these steps, the coupling efficiency leaves room for improvement. Ideally, a GC would be patterned and through-etched in the same step as part of the photonic circuits while yielding a comparable coupling efficiency. However, through-etched air trenches make the grating's index contrast very high. As a result, the Fresnel reflection is prohibitively high, and the coupling efficiency becomes very limited. Efforts have been made in recent years to address this issue. For example, an apodized through-etched GC achieved 35% coupling efficiency with a 1 dB bandwidth of 47 nm at 1536 nm.[14] However, index matching oil was needed for this design. One elegant approach is to fill air trenches with a higher index material, but such a solution may not always be available. Fortunately, artificial materials with engineered indices of refraction can also meet these requirements. For example, by using a photonic crystal structure, a 42% peak coupling efficiency was obtained with a 1 dB bandwidth of 47 nm.[3] Another interesting class of such artificial materials is the subwavelength nanostructure (SWN). Using SWN as a low index material was proposed in 2009.[15] A coupling efficiency of 43% (3.7 dB) has been reported for TM polarized light around 1550 nm.[16] Although promising results have been demonstrated for TM polarization, few reports have been made about TE polarized fiber-to-chip grating couplers at telecommunications wavelengths on a silicon-on-insulator (SOI) platform.[17]

In this Letter, we engineer the refractive index of a SWN and demonstrate a TE polarized GC achieving a 59%

[a)]Xiaochuan Xu and Harish Subbaraman contributed equally to this work.
[b)]Authors to whom correspondence should be addressed. Electronic addresses: xiaochuan.xu@mail.utexas.edu and raychen@uts.cc.utexas.edu. Fax: +1-512-471-8575.

coupling efficiency at 1551.6 nm. The 3 dB bandwidth is 60 nm. The efficiency increases 1.73 times (from 34% to 59%), and the bandwidth increases 1.5 times (from 40 nm to 60 nm) compared to the previously reported TE polarized subwavelength grating (SWG) on SOI.[17] From the manufacturing point of view, the grating can be patterned along with other photonic components through the same lithography and etching process, which significantly reduces the fabrication complexity and also enables integration on other platforms, e.g., flexible photonic components.[18]

The SWG proposed in this Letter is based on a SOI comprising of a 250 nm silicon device layer and a 1 μm buried oxide (BOX) layer. The grating is formed by periodically replacing parts of the silicon layer ($n_{si} = 3.476$) with SWN, as shown in Fig. 1(a). Optimization of the SWG with 3D finite-difference-time-domain (FDTD) is not possible because its simulation time is prohibitively long.[16] In this Letter, an alternative model is utilized. According to effective medium theory (EMT),[19] a composite medium comprising two different materials interleaved at the subwavelength scale can be approximated as a homogenous medium with an effective refractive index between these two materials. Therefore, the SWG is equivalent to the conventional GC shown in Fig. 1(b). The subwavelength region is regarded as a homogeneous material with an effective index n_{sub}.[15] The uniform material is then replaced with a SWN, as shown in Fig. 1(c).[3] To optimize the grating design, a 2D simulation package CAMFR, which is based on the eigenmode expansion technique,[20] is utilized to search for an optimal combination of grating period Λ_G and n_{sub} giving the highest coupling efficiency to air through the SWG. The duty cycle of the grating is optimized to be 50%, and 25 periods are employed. The grating region is 10 μm wide and 17.1 μm long. These dimensions match well with the mode size of a single mode fiber.[3] An exhaustive parameter sweep shows that the maximum coupling efficiency to air is 72% with an emitting angle of 9.4° when $\Lambda_G = 0.685$ μm and $n_{sub} = 2.45$, as indicated in Fig. 2(a). The corresponding coupling efficiency to air versus wavelength is shown in Fig. 2(b) (red curve). To verify the design, 2D FDTD simulations of the grating are also performed, and its results match with those obtained by CAMFR with a discrepancy within 2%. The

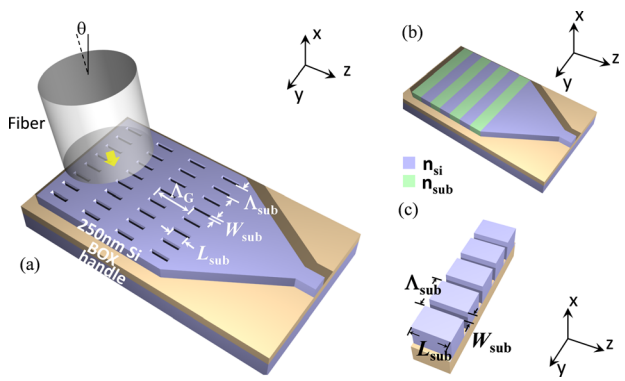

FIG. 1. (a) Schematic of the proposed SWG. (b) The equivalent conventional GC. The trenches are filled with SWN of refractive index n_{sub}. (c) Schematic of the SWN. The refractive index of the material can be controlled by tuning the width W_{sub} of the rectangular air hole and the period Λ_{sub} of the subwavelength structure.

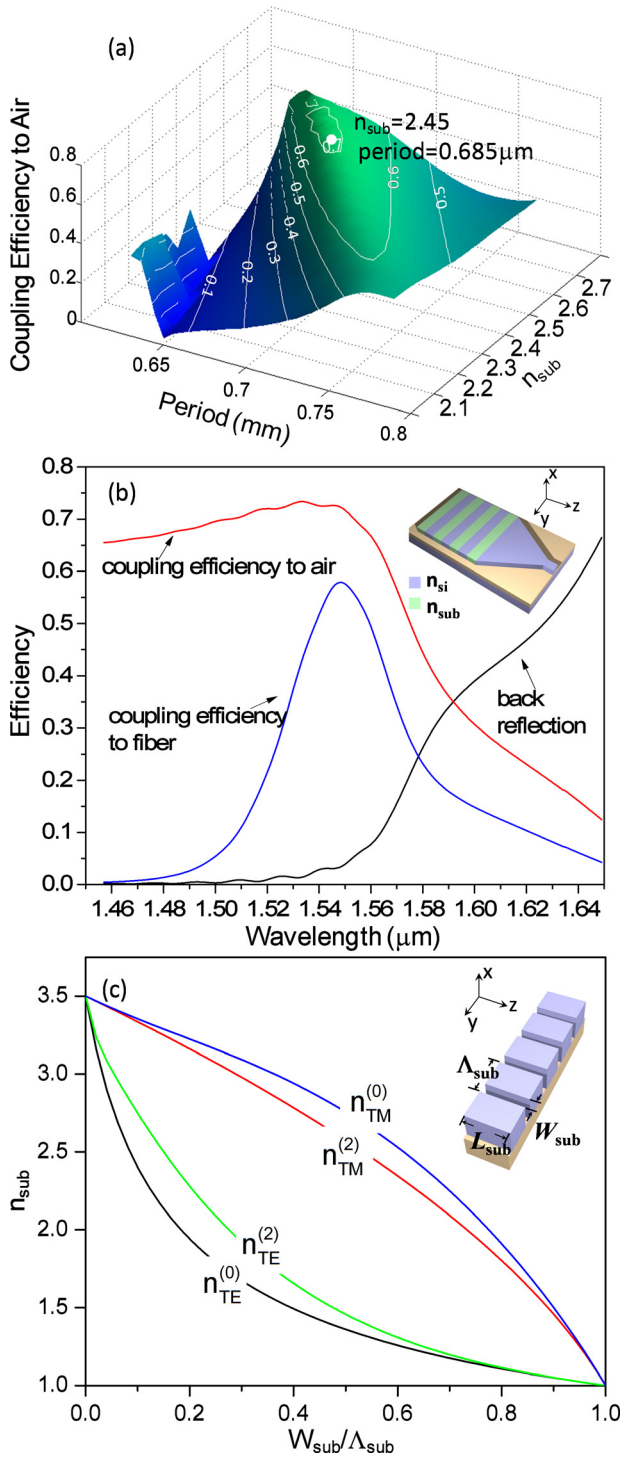

FIG. 2. (a) Coupling efficiency to air as a function of grating period Λ_G and the effective refractive index n_{sub} of the subwavelength structure. The highest coupling efficiency to air (white dot) is obtained when Λ_G is 0.685 μm and n_{sub} is 2.45. (b) Coupling efficiency to air (red), coupling efficiency to fiber (blue), and back reflection (black) from the simplified structure shown in the inset. (c) Refractive index of the SWN for different filling factors, calculated by EMT with zeroth-order and second-order approximations when Λ_{sub} is 300 nm.

coupling efficiency to a fiber, shown by the blue curve in Fig. 2(b), is evaluated by calculating the overlap integral with the Gaussian mode in a single mode fiber. Since the width of the grating is much larger than its height, decoupled 3D modes can be established in the y and z directions.[15] Since the y dependent overlap integral is close to 1,[21] the

overlap integral can be simplified to an integration along the z direction. The reflection back into the waveguide is around 3.8% at the wavelength of 1550 nm, as shown by the black curve in Fig. 2(b). The design is used for both input and output couplings. The 2D FDTD shows that the difference between input and output coupling efficiency is negligible.

Theoretically, any SWN (e.g., photonic crystals) with an effective refractive index of 2.45 may be used to "fill" the low index regions of a periodic structure, which is a grating in our case. However, as indicated in Fig. 2(a), the coupling efficiency heavily relies on n_{sub}, so a precise control of n_{sub} is crucial for achieving high coupling efficiency. In this Letter, a thoroughly investigated 1D stratified structure is chosen, so that the refractive index of the SWN can be precisely controlled.[22] As shown in Fig. 1(c), silicon and air slices are periodically laminated along the y direction. The guided wave propagation direction is parallel to the layers (z direction) and the electric field is perpendicular to the layers (y direction). In this configuration, the refractive indices of SWN for TE and TM can be calculated through Eqs. (1) and (2) that are shown below:[22]

$$\mathrm{TE}: \frac{\sqrt{n_{si}^2 - n_{TE}^2}}{n_{si}^2}\tan\left(\frac{\pi\sqrt{n_{si}^2 - n_{TE}^2}(\Lambda_{sub} - W_{sub})}{\lambda}\right) = -\frac{\sqrt{n_{hole}^2 - n_{TE}^2}}{n_{hole}^2}\tan\left(\frac{\pi\sqrt{n_{hole}^2 - n_{TE}^2}W_{sub}}{\lambda}\right), \quad (1)$$

$$\mathrm{TM}: \sqrt{n_{si}^2 - n_{TM}^2}\tan\left(\frac{\pi\sqrt{n_{si}^2 - n_{TM}^2}(\Lambda_{sub} - W_{sub})}{\lambda}\right) = -\sqrt{n_{hole}^2 - n_{TM}^2}\tan\left(\frac{\pi\sqrt{n_{hole}^2 - n_{TM}^2}W_{sub}}{\lambda}\right), \quad (2)$$

where n_{TE} and n_{TM} are the refractive indices of SWN for TE and TM polarizations, respectively. n_{si} and n_{hole} are the refractive indices of the silicon and the material in the holes, respectively. In our design, the holes are filled with air ($n_{hole} = 1$). Λ_{sub} is the period of the SWN, and W_{sub} is the width of the rectangular air holes. The filling factor of the SWN is defined as $f_{sub} = W_{sub}/\Lambda_{sub}$. As the transcendental Eqs. (1) and (2) do not have explicit analytical solution, polynomial expansion is exploited to approximate the tangent function. The n_{sub} versus f_{sub} based on zeroth-order and second-order approximations are illustrated in Fig. 2(c). The zeroth-order approximations are accurate only under the condition that along any arbitrary direction, the change in the electromagnetic field within a distance of Λ_{sub} is sufficiently small.[22] The condition can be formulated as $2\pi n_{eff}\Lambda_{sub}/\lambda \ll 1$. Here, n_{eff} is the mode effective index in the silicon slab waveguide with 250 nm thickness. For TE polarization, the corresponding f_{sub} for $n_{sub} = 2.45$ is ~0.09 according to the first-order approximation. The smallest W_{sub} that can be fabricated is ~40 nm. Thus, Λ_{sub} becomes close to the wavelength inside the slab waveguide. The zeroth-order approximations, therefore, are no longer applicable.[23] Including second-order expansion terms can improve the accuracy of the approximation as long as the permittivity of one material is not vastly different from the other.[16,17,22] Fig. 2(c) confirms that the first-order approximation underestimates the refractive index by 0.33 when the filling factor f_{sub} is 20%. Thus, the second-order approximation is used in this Letter. Considering fabrication yield and repeatability limitations, the trench width is fixed to 80 nm with a corresponding Λ_{sub} of 388 nm.

The designed GC is fabricated using electron beam lithography (EBL) and RIE. The top view and the cross view scanning electron microscopy (SEM) images of the fabricated grating are shown in Fig. 3. A magnified view of the air holes is shown in the inset of Fig. 3(a). The GC is characterized by measuring the fiber-to-waveguide-to-fiber insertion loss. The measurement setup is shown in Fig. 4(a). The input and output fibers are mounted on two 10° wedges, which are in turn mounted on rotating stages. The tilt angle can be adjusted from 0° ~ 20°. For this design, both the input and output fibers are tilted ~9.4° from normal incidence. The fiber positions are controlled by two xyz stages. A camera is mounted at a 45° angle to visually aid alignment. The input fiber is a polarization maintaining fiber (PMF), and the polarization is controlled via a polarization controller (PC). Light is coupled into an 8 mm long, 2.5 μm wide waveguide via a pair of grating couplers. Since the fundamental mode contains most of the power, the existence of higher order modes has negligible effects on the testing results. A pair of linear waveguide tapers, each with a length of 500 μm, is utilized to bridge the 10 μm wide grating region to the waveguide. The coupling efficiency is extracted assuming equal coupling efficiencies for both gratings. The transmission spectrum, as shown in Fig. 4(b), is measured with a broad band amplified spontaneous emission (ASE) source. The peak efficiency is measured to be 59% (−2.29 dB). The peak wavelength shifts to 1551.6 nm possibly due to fabrication errors. The 1 dB and 3 dB bandwidths are 32 nm and 60 nm, respectively. The Fabry-Perot fringes near the peak wavelength are ~0.3 dB in magnitude, indicating low back reflection. It is much smaller than conventional through-etched GC due to the SWN not only reducing the Fresnel reflection and also functioning as a destructive interference enhancer to reduce the reflection at the interface of the grating and free space.[16] The efficiency increases 1.73 times (from 34% to 59%), and the bandwidth increases 1.5 times (from 40 nm to 60 nm) compared to the previously reported TE polarized SWG on SOI.[17] The performance enhancement is due to the fact that the refractive index of the SWN is more precisely controlled compared to the previously reported GC.[17] The bandwidth can be further extended

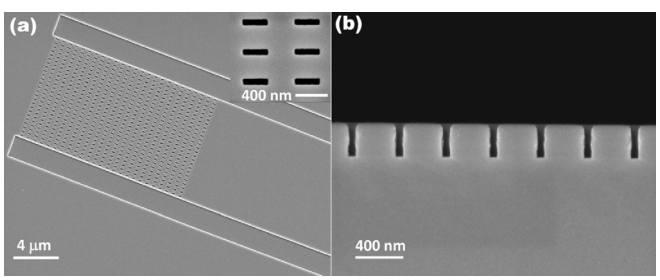

FIG. 3. (a) SEM images of the fabricated GC. Inset: the magnified view of the air holes. (b) The cross section of the rectangular air holes.

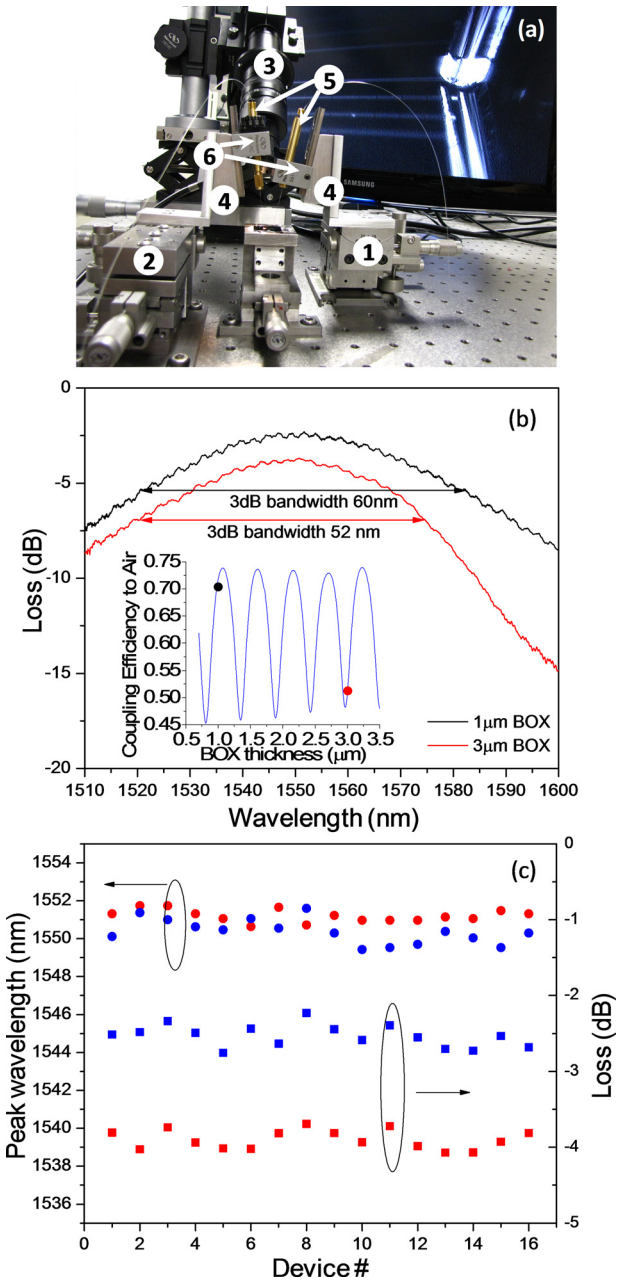

FIG. 4. (a) Testing set up. (1) Tilting stage; (2) xyz stage; (3) 45° tilted camera; (4) 10° wedges; (5) fiber chuck; and (6) chuck holder. (b) The measured transmission of the grating fabricated on the SOI with 1 μm BOX (black) and 3 μm BOX (red). Inset: Coupling efficiency to air vs. BOX thickness. (c) The peak wavelengths (dots) and the coupling losses (squares) of the fabricated 32 grating pairs on SOI with 1μm (blue) and 3μm (red) BOXs.

through increasing the tilt angle.[24] In this manner, back reflections may also be further suppressed.[16] The high efficiency of the grating also benefits from destructive interference in the BOX layer. Due to the interference effects from the downward diffracted light beam, the waveguide to free space coupling efficiency has a strong periodic dependence on the BOX thickness. The coupling efficiency could vary by as much as 30%, as illustrated in the inset of Fig. 4(b). The commercially available 1 μm BOX is close to the optimum thickness yielding the highest coupling efficency to air efficiency. For comparison, the same design is also fabricated on an SOI with a 3 μm BOX, which is close to the lowest point in the coupling efficiency to air curve shown in the inset of Fig. 4(b). For the 3 μm BOX SWG, the measured peak efficiency is 42.8% (−3.69 dB) at 1550.7 nm with 1 dB and 3 dB bandwidths of 28 nm and 52 nm, respectively. As expected, the performance is worse than that of 1 μm BOX but is still acceptable compared to recently reported gratings. To verify fabrication repeatability, 32 grating pairs, with 16 pairs on each of the 1 μm and the 3 μm BOX chips are fabricated. The measured peak wavelengths and coupling efficiencies are shown in Fig. 4(c). Peak wavelength and power vary by 1.1 nm and 0.38 dB for 3 μm BOX devices and 2.2 nm and 0.52 dB for 1 μm BOX devices, demonstrating acceptable consistency.

In conclusion, we proposed and demonstrated a through etched SWG coupler, which can be patterned together with photonic components without additional patterning steps. The grating achieves a peak coupling efficiency of 59% with a 3 dB bandwidth of 60 nm on a 1 μm BOX SOI. This performance is competitive to gratings requiring at least one extra etching step. Testing results of 32 grating pairs show very consistent performance.

This research is supported by the AFOSR Small Business Technology Transfer (STTR) under Grant FA9550-11-C-0014 and the AFOSR Multi Disciplinary University Research Initiative (MURI), under Grant FA9550-08-1-0394, monitored by Dr. Gernot Pomrenke.

[1]M. Asghari and A. V. Krishnamoorthy, Nat. Photonics **5**(5), 268 (2011).
[2]M. Lipson, J. Lightwave Technol. **23**(12), 4222 (2005).
[3]L. Liu, M. Pu, K. Yvind, and J. M. Hvam, Appl. Phys. Lett. **96**(5), 051126 (2010).
[4]T. Shoji, T. Tsuchizawa, T. Watanabe, K. Yamada, and H. Morita, Electron. Lett. **38**(25), 1669 (2002).
[5]S. J. McNab, N. Moll, and Y. A. Vlasov, Opt. Express **11**(22), 2927 (2003).
[6]M. Pu, L. Liu, H. Ou, K. Yvind, and J. M. Hvam, Opt. Commun. **283**(19), 3678 (2010).
[7]V. R. Almeida, R. R. Panepucci, and M. Lipson, Opt. Lett. **28**(15), 1302 (2003).
[8]P. Cheben, D. X. Xu, S. Janz, and A. Densmore, Opt. Express **14**(11), 4695 (2006).
[9]P. Cheben, P. J. Bock, J. H. Schmid, J. Lapointe, S. Janz, D. X. Xu, A. Densmore, A. Delage, B. Lamontagne, and T. J. Hall, Opt. Lett. **35**(15), 2526 (2010).
[10]D. Taillaert, F. Van Laere, M. Ayre, W. Bogaerts, D. Van Thourhout, P. Bienstman, and R. Baets, Jpn. J. Appl. Phys., Part 1 **45**(8A), 7 (2006).
[11]Y. Tang, Z. Wang, L. Wosinski, U. Westergren, and S. He, Opt. Lett. **35**(8), 1290 (2010).
[12]G. Roelkens, D. Vermeulen, D. Van Thourhout, R. Baets, S. Brision, P. Lyan, P. Gautier, and J. M. Fedeli, Appl. Phys. Lett. **92**(13), 131101 (2008).
[13]F. Van Laere, G. Roelkens, M. Ayre, J. Schrauwen, D. Taillaert, D. Van Thourhout, T. F. Krauss, and R. Baets, J. Lightwave Technol. **25**(1), 151 (2007).
[14]M. Antelius, K. B. Gylfason, and H. Sohlström, Opt. Express **19**(4), 3592 (2011).
[15]R. Halir, P. Cheben, S. Janz, D.-X. Xu, Í. Molina-Fernández, and J. G. Wangüemert-Pérez, Opt. Lett. **34**(9), 1408 (2009).
[16]R. Halir, P. Cheben, J. H. Schmid, R. Ma, D. Bedard, S. Janz, D. X. Xu, A. Densmore, J. Lapointe, and Í. Molina-Fernández, Opt. Lett. **35**(19), 3243 (2010).
[17]C. Xia and H. K. Tsang, Photon. J. IEEE **1**(3), 184 (2009).
[18]X. Xu, H. Subbaraman, A. Hosseini, C.-Y. Lin, D. Kwong, and R. T. Chen, Opt. Lett. **37**(6), 1020 (2012).
[19]P. Yeh, A. Yariv, and C.-S. Hong, J. Opt. Soc. Am. **67**(4), 423 (1977).
[20]P. Bienstman and R. Baets, Opt. Quantum Electron. **33**(4), 327 (2001).
[21]D. Taillaert, P. Bienstman, and R. Baets, Opt. Lett. **29**(23), 2749 (2004).
[22]S. M. Rytov, Sov. Phys. JETP **2**(3), 10 (1956).
[23]X. Chen and H. K. Tsang, Opt. Lett. **36**(6), 796 (2011).
[24]C. R. Doerr, C. Long, C. Young-Kai, and L. L. Buhl, IEEE Photon. Technol. Lett. **22**(19), 1461 (2010).